

Cocrystal Polymorphic Control by Nanodroplet and Electrical Confinement

Luis Padrela^[a], Bernardo Castro-Dominguez^[b], Ahmad Ziaee^[a], Barry Long^[a], Kevin M Ryan^[a], Gavin Walker^[a] and Emmet O'Reilly^{*[a]}

Electronic Supporting Information (ESI)

Conventional Spray-drying

Samples produced via conventional spray-drying were generated utilizing a commercial Büchi B-290 mini spray-dryer, described in detail in the literature ^[1]. The unit contained a 2-fluid nozzle with 0.7 mm cap, which was used for atomization. Solid particles were collected by a high efficiency cyclone. All the powders generated were transferred to a desiccator immediately before their characterization.

Electrospraying

All electrospaying work was carried out on a custom built electrospaying/electrospinning device as shown in Figure S1. The electrospaying units consisted of a 25 ml plastic syringe with a stainless steel metallic needle of 0.43 mm in diameter. A syringe pump was used to continuously push the precursor solution out of the syringe while the syringe needle was connected to a high voltage power supply (Bertan, Series 230). Aluminium foils were ground-connected and used to collect the electrospayed co-crystals. The foils were positioned at a distance of 14 cm from the tip of the needle.

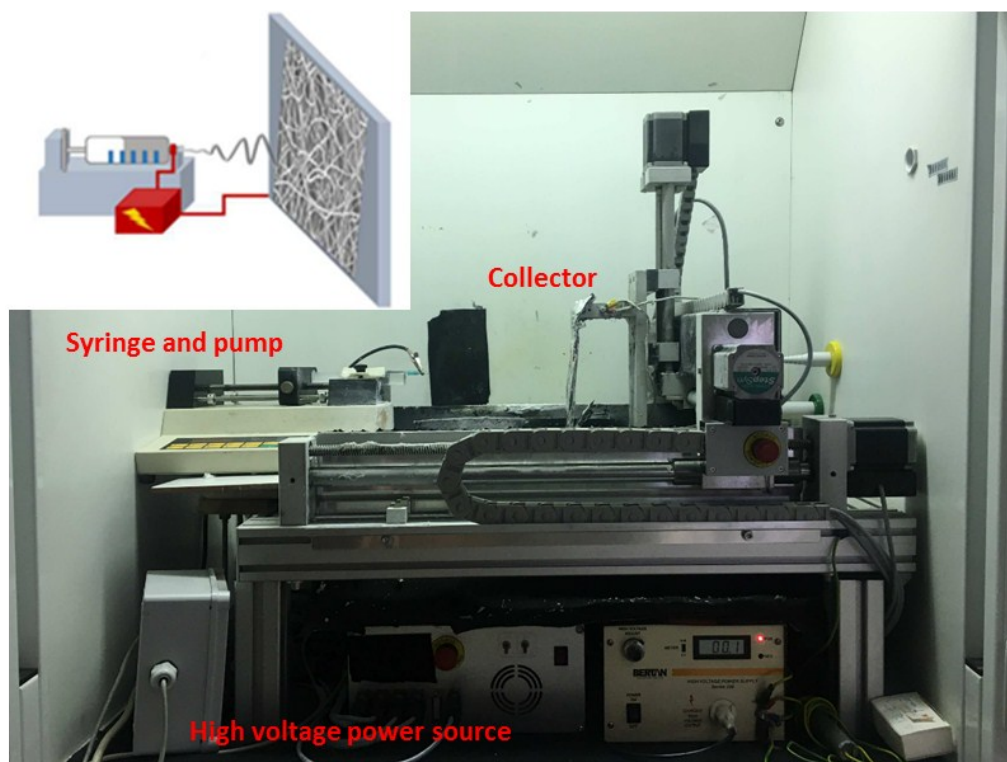


Figure S1: The electrospaying/electrospinning unit utilised for electro-confinement of the crystallization precursor and a graphic of the process (insert).

Supercritical CO₂ nano spray- drying

A custom built unit was utilized to nano spray-dry the precursor solution containing CBZ and SAC. Figure S2 represents a schematic of the unit, where supercritical CO₂ was produced by pressurizing the gas into a vessel regulated by a metering valve. Gas was compressed by a Teledyne ISCO 260D pump and the pressure was determined using a pressure transducer (Omega model PX603). The CO₂ was then allowed to flow into a high-pressure stainless steel storage vessel to reach the set temperature inside the temperature-controlled (monitored by a T-type thermocouple) air chamber. Afterwards, the supercritical CO₂ flowed to the high-pressure nozzle in the spray drying apparatus where it mixed with the CBZ-SAC solutions. A coaxial nozzle was used to mix the supercritical fluid and the precursor solution into the precipitator vessel. The products were collected in by filter located at the outlet of the precipitator. All samples were stored in a desiccator prior to characterization.

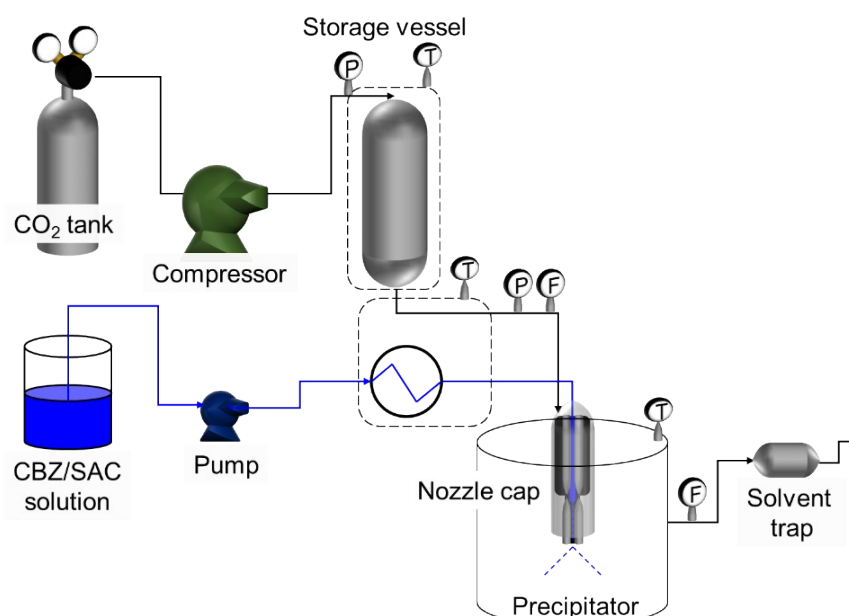


Figure S2: Schematic of the supercritical CO₂ nano spray-dryer.

Powder X-ray diffraction

An X'pert PRO X-ray diffractometer (PANalytical,) with mono-chromatized Cu K α radiation ($\lambda = 0.15405$ nm) was used for XRD analysis. The High Score Plus software was used for post analyses. The employed X-ray generator setting was 40 kV and 40 mA. Data were collected over the 2θ range of $5-50^\circ$, with a step size of $0.02^\circ \cdot \text{step}^{-1}$ and a step time of $40 \text{ s} \cdot \text{step}^{-1}$.

Differential scanning calorimetry

A PerkinElmer DSC 8500 equipped with a refrigerated cooling accessory (PerkinElmer, Workingham) using nitrogen ($30 \text{ mL} \cdot \text{min}^{-1}$) as the purge gas was used to study all the samples. The instrument was calibrated at heating rates of $5^\circ \text{C} \cdot \text{min}^{-1}$ using high purity indium and zinc to standardise the temperature and heat flow signals. Samples (~ 5.0 mg) were weighed and placed in crimped DSC pans, then ramped from 20 to 190°C at $5^\circ \text{C} \cdot \text{min}^{-1}$. Figure S3 shows the DSC profiles of all the

samples generated in this work. Diverse polymorphs show different decomposition energies at different temperatures. For instance, the onset temperature of Form I occurred at 172 °C, while the onset of Form II at 168 °C; as shown before in the pertinent literature.² In addition there was no indication of residual solvent in any of the CBZ-SAC samples. Figure S3 shows the lack of polymorphic exclusivity and selectivity of the solvent evaporation and the conventional spray-drying methods. Furthermore, the presence of exclusive Form I or II in nano spray-drying and electro spraying is clearly observed.

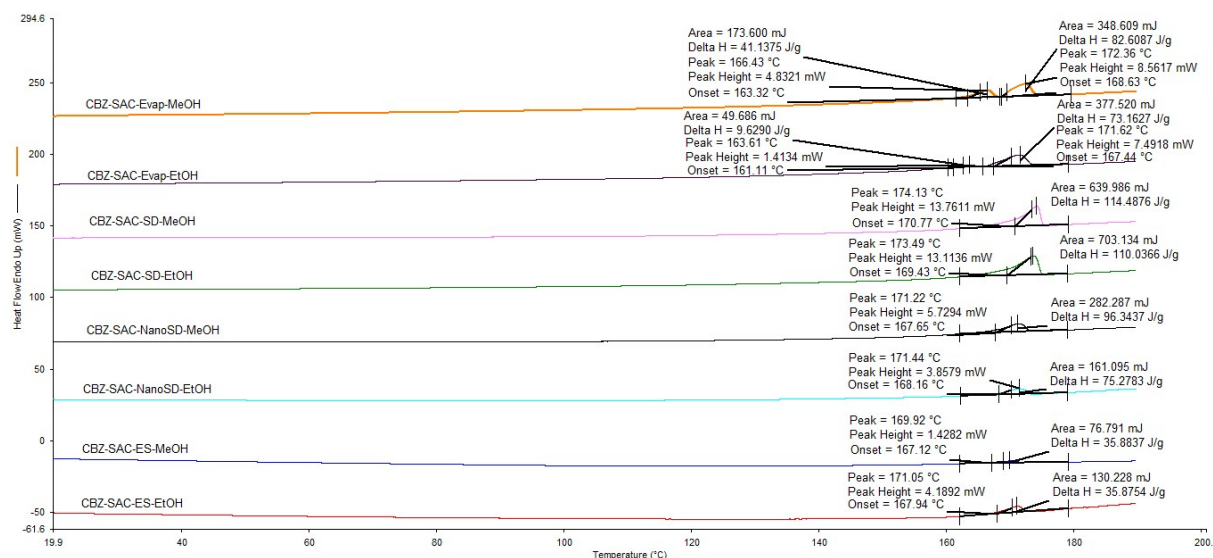


Figure S3: DSC of CBZ-SAC cocrystal samples produced using different methods.

Fourier transform infrared spectroscopy (FTIR)

A Perkin-Elmer Spectrum 100 FTIR spectrometer was used to obtain the spectra of the samples generated. The spectra was collected at room temperature at wavelengths of 4000–650 cm^{-1} . The samples were placed and 128 scans were collected for each sample at a resolution of 4.00 cm^{-1} . Figure S4 shows the spectra of CBZ-SAC cocrystals synthesized via evaporation and electro spraying from a methanol solution.

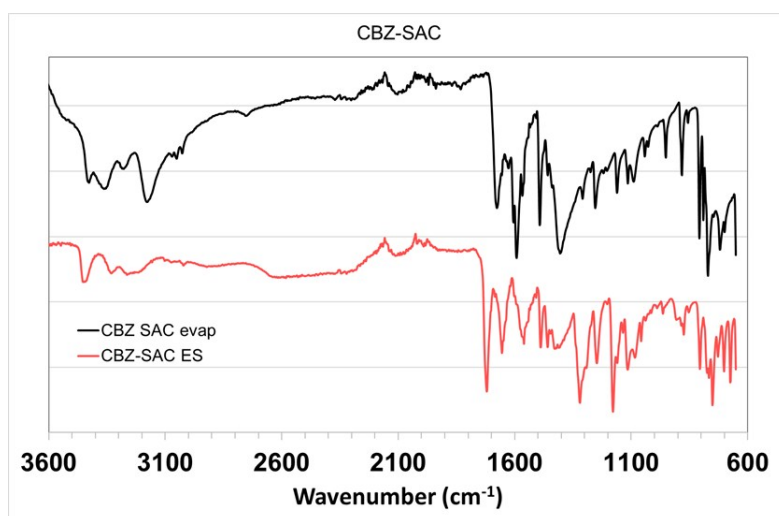


Figure S4: FTIR spectra of CBZ-SAC cocrystals synthesized via solvent evaporation and electro spraying from a methanol solution.

Electron mapping

The structure of the carbamazepine and saccharin molecules were optimized via Gaussian 09 software package². Density functional theory (DFT) was used to optimize the molecular structures. The 6-311 G basis set³ was applied to all atoms in the optimization process. Avogadro software suit⁴ was employed in mapping the electron densities. Ab initio simulations were carried out on Irish Centre for High End Computing (ICHEC).

References

¹ A. Ziaee, A.B. Albadarin, L. Padrela, A. Faucher, E. O'Reilly, G. Walker, *Eur. J. Pharm. Biopharm.*, 2017, **120**, 43–51.

² Gaussian 09, Revision A.02, M. J. Frisch, G. W. Trucks, H. B. Schlegel, G. E. Scuseria, M. A. Robb, J. R. Cheeseman, G. Scalmani, V. Barone, G. A. Petersson, H. Nakatsuji, X. Li, M. Caricato, A. Marenich, J. Bloino, B. G. Janesko, R. Gomperts, B. Mennucci, H. P. Hratchian, J. V. Ortiz, A. F. Izmaylov, J. L. Sonnenberg, D. Williams-Young, F. Ding, F. Lipparini, F. Egidi, J. Goings, B. Peng, A. Petrone, T. Henderson, D. Ranasinghe, V. G. Zakrzewski, J. Gao, N. Rega, G. Zheng, W. Liang, M. Hada, M. Ehara, K. Toyota, R. Fukuda, J. Hasegawa, M. Ishida, T. Nakajima, Y. Honda, O. Kitao, H. Nakai, T. Vreven, K. Throssell, J. A. Montgomery, Jr., J. E. Peralta, F. Ogliaro, M. Bearpark, J. J. Heyd, E. Brothers, K. N. Kudin, V. N. Staroverov, T. Keith, R. Kobayashi, J. Normand, K. Raghavachari, A. Rendell, J. C. Burant, S. S. Iyengar, J. Tomasi, M. Cossi, J. M. Millam, M. Klene, C. Adamo, R. Cammi, J. W. Ochterski, R. L. Martin, K. Morokuma, O. Farkas, J. B. Foresman, and D. J. Fox, Gaussian, Inc., Wallingford CT, 2016.

³ (a) A. D. McLean, G. S. Chandler, *J. Chem. Phys.*, 1980, **72**, 5639-48., (b) K. Raghavachari, J. S. Binkley, R. Seeger, J. A. Pople, *J. Chem. Phys.*, 1980, **72**, 650-54.

⁴ M.D. Hanwell, D.E Curtis, D.C. Lonie, T. Vandermeersch, E. Zurek, G.. Hutchison, *J. Chemoinf.*, 2012, **4**, 17.